OPTICAL POLARIZATION OBSERVATIONS OF NGC 6231: EVIDENCE FOR A PAST SUPERNOVA FINGERPRINT[1]

CARLOS FEINSTEIN,[2] RUBEN MARTÍNEZ, M. MARCELA VERGNE,[2]
GUSTAVO BAUME,[2] AND RUBÉN VÁZQUEZ[2]
Facultad de Ciencias Astronómicas y Geofísicas, Paseo del Bosque,
1900 La Plata, Argentina
Received 2003 May 5; accepted 2003 July 30

ABSTRACT

We present the first linear multicolor polarization observations for a sample of 35 stars in the direction of the Galactic cluster NGC 6231. We have found a complex pattern in the angles of the polarimetric vectors. Near the core of this cluster the structure shows a semicircular pattern that we have interpreted as a reorientation of the dust particles showing the morphology of the magnetic field. We propose that a supernova event occurred some time ago and produced a shock on the local ISM. We discuss in this paper independent confirmations of this event, both from the studies on the diffuse interstellar absorptions and the results of the pre–main-sequence stars. We also show that a supernova is supported by the evolutionary status of the cluster.

Subject headings: dust, extinction — open clusters and associations: individual (NGC 6231) — polarization — supernova remnants

1. INTRODUCTION

Polarimetric techniques are very useful tools for finding important information ($P_{\lambda \max}$, $\lambda_{\max}$, magnetic field direction, etc.) from the dust located in front of a star (or a luminous object) or from dust located inside a stellar cluster. Young open clusters are very good candidates on which to carry out polarimetric observations, because previous photometric and spectroscopic studies of these clusters give detailed information of the main sequence, so we can characterize the physical parameters of the member stars (age, distance, memberships, etc.) in order to study the extinction of the dust in the direction of the cluster and within the cluster.

For example, from the study of the $P_{\lambda \max}$ versus the E_{B-V} of each star of a cluster, it is possible to find the polarimetric components of the extinction produced by Galactic dust located between the Sun and the cluster (e.g., Tr 27; Feinstein et al. 2000). By subtracting the effect of this dust on the line of sight from the data, it is possible to study the component associated with the internal extinction of the cluster. In addition to this valuable information, stars with intrinsic polarimetric properties can be isolated. The angle of the polarization vector is an estimator of the direction of the Galactic magnetic field. By observing member and non-member stars (foreground and background), the direction of the magnetic field toward the cluster at several distances can be inferred.

In a typical open cluster the polarimetric data show, for "normal" stars (that is, not considering stars with intrinsic polarization), a distribution of angles that can be described by a mean fixed value that characterizes the cluster. The polarization angles of the cluster members show some scatter ($\sim 10°$ or less) over this mean angle, mainly because of density inhomogeneities in the dust along the line of sight to the cluster and inhomogeneities of the dust inside the cluster to the intrinsic polarimetric properties of the stars and also because of more complex magnetic field structures. For example, in Tr 27, the polarimetric data show a mean angle of $\theta \sim 30°$ for the cluster with a FWHM of $\sim 10°$ (Feinstein et al. 2000); in Ara OB1 the polarimetric observations give a FWHM of $\sim 9°.9$ for NGC 6167, $\sim 13°.1$ for NGC 6193, and $\sim 9°.5$ for NGC 6204 (Waldhausen, Martínez, & Feinstein 1999). In the case of Stock 16 (Feinstein et al. 2002), the FWHM is $6°.7$, which seems to be slightly smaller than the other clusters.

NGC 6231 ($l = 345°.5$, $b = 1°.2$) is known in the literature to be one of the youngest open clusters in the Galaxy and one of the brightest in the southern hemisphere. The cluster is embedded in an extended system of O and early B stars, namely, the very young association Sco OB1, which contains the ring-shaped H II region IC 4678 centered on NGC 6231. Usually, NGC 6231 is considered the nucleus of Sco OB1 (Perry, Hill, & Christodoulou 1991). Its age determinations range between 3×10^6 yr (Mermilliot & Maeder 1986) and 6.9×10^6 yr (Perry et al. 1991). It is known as one of the richest open clusters, containing WR stars, β Cepheid variables, and more than 100 O and B stars (Shobbrook 1983). According to photometric CCD observations of Sung, Bessell, & Lee (1998) and of Baume, Vázquez, & Feinstein (1999), there is evidence of a population of pre–main-sequence stars (PMS). The distance obtained by deep CCD photometry by Baume et al. (1999) locates the cluster NGC 6231 at 1990 ± 200 pc from the Sun.

The average visual extinction toward the cluster is about $A_V \sim 1.4$ (Balona & Laney 1995; Baume et al. 1999). According to Raboud, Cramer, & Bernasconi (1997), in the northern part of the cluster, the absorption is constant, but it increases from the central part toward the south. A similar trend, but less pronounced, is observed from west to east in the southern part. Part of the absorption suffered by the

light from the cluster stars is caused by matter within the distance interval 100–1300 pc from the Sun (Perry et al. 1991), but the field shows a relatively good transparency between about 400 and 1000 pc at a constant value averaging $A_V = 0.75$ mag (Raboud et al. 1997).

2. OBSERVATIONS

The bulk of the observations were obtained on two observing runs. The first one was performed during 1995 (May 30 to June 3). The second one was on three nights in 2001 (August 17–20). Two more runs in 2002 May and 2002 August were used for reobserving and checking some stars. All runs were carried out using the five-channel photo-polarimeter of the Torino Astronomical Observatory (Scaltriti et al. 1989) attached to the 2.15 m telescope at the Complejo Astronómico El Leoncito (San Juan, Argentina). Polarimetric measurements have been made for 36 stars to the cluster NGC 6231. Most of them were observed through the Johnson broadband *UBVRI* filters

$$(\lambda_{U,\,\mathrm{eff}} = 0.360 \ \mu\mathrm{m} \ , \ \lambda_{B,\,\mathrm{eff}} = 0.440 \ \mu\mathrm{m} \ ,$$
$$\lambda_{V,\,\mathrm{eff}} = 0.530 \ \mu\mathrm{m} \ , \ \lambda_{R,\,\mathrm{eff}} = 0.690 \ \mu\mathrm{m} \ ,$$
$$\lambda_{I,\,\mathrm{eff}} = 0.830 \ \mu\mathrm{m}) \ .$$

Our results are listed in Table 1, which shows, in a self-explanatory format, the stellar identification as given by Seggewiss (1968), the average of the percentage of polarization (P_λ), and the position angle of the electric vector (θ_λ) observed through each filter, with their respective mean errors.

The Torino polarimeter collects data for all the filters simultaneously (*UVBRI*), so all the wavebands have the same exposure times, and the S/N varies between filters. Therefore, the values from different filters may be of different quality. Observations whose values are not over the 3 σ error level were discarded, and they are neither reported in Table 1 nor used in this work.

Several standard stars for null polarization and for the zero point of the polarization position angle were measured for calibration purposes. At least three standard angle stars were measured every night at different times. Errors were handled as described by Maronna, Feinstein, & Clocchiatti (1992). In order to verify the lack of systematic differences between both main runs, we reobserved a common group of stars in the second run.

Three other bright stars were observed previously by Serkowski, Mathewson, & Ford (1975): these are HD 152234 (star 290), HD 152235, and HD 152248. Although in that paper no observation errors were given, their data (polarization and angle) are very similar to those reported in the present paper (see Table 2).

To look for nearby objects, the observed stars were checked with the *Hipparcos*/Tycho Catalog data. Stars 80, 110, 112, 220, 290, and HD 152248 were included in these catalogs but are so far away from the Sun that no useful parallax measures could be obtained.

3. RESULTS

Figure 1 shows the sky projection of the *V*-band polarization for the stars in NGC 6231. The dot-dashed line indicates the Galactic parallel $b = 1°.1$. The first striking

TABLE 1
POLARIMETRIC OBSERVATIONS OF STARS IN NGC 6231

Filter	$P_\lambda \pm \epsilon_P$ (%)	$\theta_\lambda \pm \epsilon_\theta$ (deg)
Star 1		
U	1.24 ± 0.42	58.4 ± 9.3
B	0.84 ± 0.19	47.9 ± 6.5
V	0.66 ± 0.17	25.5 ± 7.1
R	0.94 ± 0.22	26.3 ± 6.6
I	0.99 ± 0.47	32.7 ± 12.8
Star 6		
B	0.33 ± 0.07	31.6 ± 6.2
V	0.34 ± 0.06	15.5 ± 5.3
R	0.35 ± 0.05	10.0 ± 3.9
I	0.34 ± 0.10	17.0 ± 8.3
Star 16		
V	0.36 ± 0.07	20.8 ± 5.7
R	0.37 ± 0.07	15.6 ± 5.0
I	0.31 ± 0.07	24.4 ± 6.3
Star 34		
B	1.36 ± 0.12	37.4 ± 2.5
V	1.37 ± 0.14	28.4 ± 2.8
R	1.45 ± 0.17	21.7 ± 3.3
I	1.60 ± 0.24	24.8 ± 4.2
Star 70		
U	1.77 ± 0.09	130.1 ± 1.4
B	0.94 ± 0.08	157.3 ± 2.4
V	1.68 ± 0.07	103.4 ± 1.2
R	1.48 ± 0.07	146.9 ± 1.3
I	1.90 ± 0.10	167.8 ± 1.4
Star 73		
U	1.82 ± 0.09	140.6 ± 1.4
B	1.59 ± 0.07	164.7 ± 1.2
V	1.08 ± 0.08	101.6 ± 2.1
R	1.87 ± 0.05	154.5 ± 0.8
I	2.53 ± 0.07	169.5 ± 0.8
Star 80		
U	0.89 ± 0.15	118.9 ± 4.7
B	0.97 ± 0.09	131.2 ± 2.8
V	1.02 ± 0.10	121.9 ± 2.9
R	1.05 ± 0.09	117.1 ± 2.4
I	0.79 ± 0.16	120.3 ± 5.5
Star 102		
U	0.69 ± 0.12	24.9 ± 5.0
B	0.78 ± 0.07	17.4 ± 2.5
V	0.85 ± 0.10	8.0 ± 3.3
R	0.85 ± 0.10	1.3 ± 3.2
I	0.73 ± 0.11	4.8 ± 4.2
Star 105		
U	1.06 ± 0.12	93.2 ± 3.4
B	1.19 ± 0.07	88.8 ± 1.7
V	1.09 ± 0.14	83.4 ± 3.6
R	1.03 ± 0.09	88.3 ± 2.4
I	0.99 ± 0.14	83.9 ± 4.1

TABLE 1—*Continued*

Filter	$P_\lambda \pm \epsilon_P$ (%)	$\theta_\lambda \pm \epsilon_\theta$ (deg)
Star 110		
U..........................	0.60 ± 0.14	98.7 ± 6.8
B..........................	0.40 ± 0.13	102.4 ± 9.0
V..........................	0.38 ± 0.12	90.6 ± 8.5
R..........................	0.43 ± 0.10	85.1 ± 6.4
Star 112		
U..........................	0.46 ± 0.11	105.1 ± 6.6
B..........................	0.51 ± 0.11	107.8 ± 5.9
V..........................	0.62 ± 0.09	100.1 ± 4.2
R..........................	0.50 ± 0.07	93.7 ± 4.0
I..........................	0.46 ± 0.06	99.1 ± 3.8
Star 161		
U..........................	0.29 ± 0.10	25.4 ± 9.4
B..........................	0.38 ± 0.04	41.3 ± 3.1
V..........................	0.46 ± 0.05	43.6 ± 3.4
R..........................	0.31 ± 0.05	40.8 ± 4.9
I..........................	0.13 ± 0.07	38.3 ± 14.8
Star 166		
U..........................	0.69 ± 0.20	43.9 ± 8.3
B..........................	0.69 ± 0.25	49.4 ± 9.8
V..........................	0.69 ± 0.18	44.5 ± 7.5
R..........................	0.54 ± 0.17	40.6 ± 8.9
I..........................	0.54 ± 0.24	36.5 ± 12.1
Star 184		
V..........................	0.55 ± 0.15	177.0 ± 7.6
R..........................	0.44 ± 0.13	170.3 ± 8.0
Star 189		
B..........................	0.64 ± 0.20	22.5 ± 8.5
V..........................	0.46 ± 0.11	18.4 ± 6.9
R..........................	0.41 ± 0.09	11.1 ± 6.3
Star 194		
U..........................	0.61 ± 0.14	4.1 ± 6.6
B..........................	0.69 ± 0.12	2.2 ± 4.8
V..........................	0.52 ± 0.12	174.0 ± 6.5
R..........................	0.26 ± 0.08	179.8 ± 8.7
Star 220		
U..........................	0.63 ± 0.15	116.1 ± 6.7
B..........................	0.62 ± 0.12	130.8 ± 5.4
V..........................	0.63 ± 0.14	112.7 ± 6.4
R..........................	0.65 ± 0.12	105.9 ± 5.1
I..........................	0.50 ± 0.15	109.4 ± 8.3
Star 224		
U..........................	0.41 ± 0.14	102.1 ± 9.2
B..........................	0.33 ± 0.08	108.6 ± 7.1
V..........................	0.29 ± 0.07	93.8 ± 7.0
R..........................	0.34 ± 0.07	94.3 ± 6.0
I..........................	0.28 ± 0.10	88.2 ± 9.4
Star 232		
U..........................	0.83 ± 0.18	102.6 ± 6.0
B..........................	0.94 ± 0.16	107.1 ± 4.7
V..........................	0.86 ± 0.16	100.1 ± 5.4
R..........................	0.83 ± 0.15	101.1 ± 5.1
I..........................	0.70 ± 0.10	98.4 ± 4.0

TABLE 1—*Continued*

Filter	$P_\lambda \pm \epsilon_P$ (%)	$\theta_\lambda \pm \epsilon_\theta$ (deg)
Star 238		
U..........................	0.39 ± 0.13	95.9 ± 9.1
B..........................	0.36 ± 0.12	111.9 ± 9.4
V..........................	0.36 ± 0.11	94.0 ± 8.7
R..........................	0.41 ± 0.09	89.2 ± 6.4
Star 248		
U..........................	1.77 ± 0.51	104.2 ± 7.9
B..........................	1.60 ± 0.17	116.5 ± 3.0
V..........................	1.54 ± 0.19	102.7 ± 3.6
R..........................	1.42 ± 0.25	99.9 ± 5.0
I..........................	1.28 ± 0.43	101.5 ± 9.3
Star 253		
U..........................	0.86 ± 0.14	105.7 ± 4.8
B..........................	1.06 ± 0.16	108.1 ± 4.2
V..........................	0.97 ± 0.15	98.6 ± 4.4
R..........................	0.93 ± 0.14	92.6 ± 4.2
I..........................	0.64 ± 0.22	95.5 ± 9.4
Star 254		
B..........................	0.96 ± 0.10	112.7 ± 3.0
V..........................	0.80 ± 0.14	87.8 ± 5.0
R..........................	0.83 ± 0.12	90.5 ± 4.2
Star 259		
U..........................	0.78 ± 0.13	108.2 ± 4.8
B..........................	1.00 ± 0.14	108.1 ± 3.9
V..........................	0.85 ± 0.11	109.5 ± 3.6
R..........................	0.80 ± 0.07	111.8 ± 2.6
I..........................	0.64 ± 0.14	116.8 ± 6.1
Star 261		
U..........................	0.58 ± 0.10	108.2 ± 4.9
B..........................	0.57 ± 0.15	105.9 ± 7.2
V..........................	0.52 ± 0.15	101.6 ± 7.8
R..........................	0.51 ± 0.11	102.8 ± 6.0
I..........................	0.43 ± 0.15	99.1 ± 9.4
Star 266		
U..........................	0.37 ± 0.07	49.5 ± 5.6
B..........................	0.33 ± 0.06	51.8 ± 5.3
V..........................	0.38 ± 0.08	44.7 ± 6.0
R..........................	0.37 ± 0.05	40.8 ± 4.0
I..........................	0.42 ± 0.09	36.2 ± 5.8
Star 272		
U..........................	0.65 ± 0.13	160.6 ± 5.7
B..........................	0.59 ± 0.11	168.0 ± 5.4
V..........................	0.48 ± 0.09	162.4 ± 5.0
R..........................	0.46 ± 0.08	153.6 ± 5.1
Star 286		
U..........................	0.64 ± 0.19	152.4 ± 8.2
B..........................	0.52 ± 0.08	142.8 ± 4.3
V..........................	0.35 ± 0.11	132.5 ± 8.4
R..........................	0.39 ± 0.10	128.3 ± 7.1

TABLE 1—*Continued*

Filter	$P_\lambda \pm \epsilon_P$ (%)	$\theta_\lambda \pm \epsilon_\theta$ (deg)
Star 287		
U........................	0.80 ± 0.12	133.5 ± 4.2
B........................	0.80 ± 0.10	133.6 ± 3.5
V........................	0.82 ± 0.09	137.1 ± 3.1
R........................	0.72 ± 0.11	135.5 ± 4.3
I........................	0.64 ± 0.10	133.4 ± 4.5
Star 289		
U........................	0.69 ± 0.07	135.1 ± 2.8
B........................	0.81 ± 0.08	135.4 ± 2.8
V........................	0.64 ± 0.08	132.8 ± 3.5
R........................	0.63 ± 0.08	132.0 ± 3.6
I........................	0.50 ± 0.12	132.0 ± 6.9
Star 290		
U........................	0.65 ± 0.15	172.1 ± 6.4
B........................	0.64 ± 0.13	169.3 ± 5.9
V........................	0.65 ± 0.14	157.4 ± 6.0
R........................	0.58 ± 0.13	157.1 ± 6.5
I........................	0.51 ± 0.14	163.6 ± 7.7
Star 292		
U........................	0.49 ± 0.11	123.1 ± 6.1
B........................	0.37 ± 0.09	133.4 ± 6.9
Star HD 152233		
B........................	0.66 ± 0.12	171.7 ± 5.3
V........................	0.54 ± 0.10	163.3 ± 5.4
R........................	0.60 ± 0.11	156.6 ± 5.1
Star HD 152235		
U........................	0.97 ± 0.10	105.1 ± 2.8
B........................	1.00 ± 0.09	99.7 ± 2.5
V........................	0.97 ± 0.10	101.2 ± 3.1
R........................	0.90 ± 0.04	100.6 ± 1.4
I........................	0.71 ± 0.11	95.3 ± 4.3
Star HD 152248		
U........................	0.55 ± 0.15	120.6 ± 7.6
B........................	0.49 ± 0.12	125.0 ± 6.6
V........................	0.59 ± 0.12	119.1 ± 5.9
R........................	0.49 ± 0.12	111.7 ± 6.9
I........................	0.52 ± 0.16	105.1 ± 8.3
Star CPD −47 7733		
B........................	0.31 ± 0.12	96.8 ± 10.0
V........................	0.36 ± 0.10	89.5 ± 7.9
R........................	0.38 ± 0.09	87.1 ± 6.9
I........................	0.47 ± 0.09	78.1 ± 5.3
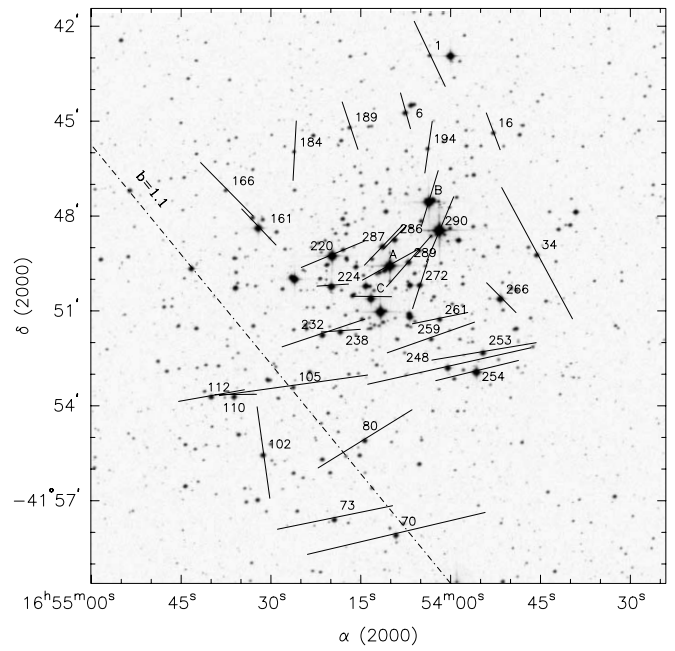
Fig. 1.—Projection of the polarization vectors (Johnson *V* filter) over the sky. *Dot-dashed line*: Galactic parallel $b = 1°1$. Star named A is HD 152248, star B is HD 152233, and star C is CPD −41 7733.

feature of this figure is the abnormal distribution of the polarization angles. Commonly, in a typical open cluster, the polarization vectors have a similar mean orientation of the polarization angle, and the individual stars show little scatter over this fixed direction. Previous studies of the five clusters indicate that this scatter is equal to or less than $10°$ of FWHM (Waldhausen et al. 1999; Feinstein et al. 2000, 2002). As seen in Figure 1, this is not the case in NGC 6231.

It is possible to classify the stars of NGC 6231 into three groups according to their location and the angle of the polarization vectors as shown in Figure 1. Stars in the northern part of the image in Figure 1 form the first group, which has vectors orientated in the direction of the Galactic disk; see, for example, stars 1, 6, 16, 184, and 189. To the south, three more stars (34, 102, and 266) also have vectors orientated with the same direction. Stars 16, 102, 184, and 189 are considered nonmembers of the cluster (Baume et al. 1999), and this fact can explain the alignment of the polarization vectors with the Galactic plane. We believe that all of this group probably consists of nonmembers or less reddened members that are closer to the Sun ("front-side stars"), and we are seeing them without the effect of the intracluster dust.

It is very noticeable that most of the polarization vectors of the stars in the inner core of the cluster seem to form part

TABLE 2

Comparison Between Serkowski et al. (1975)[1] and This Paper

HD	$P_{\text{Serkowski}}$ (%)	$\theta_{\text{Serkowski}}$ (deg)	P (%)	θ (deg)	ID (Seggewiss)
152248	0.66	112	0.59 ± 0.12	119.1 ± 5.9	...
152234	0.70	148	0.65 ± 0.14	157.4 ± 6.0	290
152235	0.92	110.4	0.97 ± 0.11	101.2 ± 2.6	...

[1] No error numbers were indicated in the Serkowski et al. 1975 paper.

of a semicircular structure, and none of them appear to be aligned with the direction of the Galactic disk. We consider these stars the second group. The third group consist of stars with their polarimetric vectors at right angles to the direction of the Galactic disk. These are stars 70, 73, 80, 105, 110, 112, 248, 253, and 254 to the south. The second group is a very unusual finding. In the next section we discuss some probable explanations based on our polarimetric observations and on data from other authors obtained with different astronomical techniques (photometry, spectroscopy, etc.).

4. ANALYSIS AND DISCUSSION

4.1. *Serkowski Law*

To analyze the data, the polarimetric observations were fitted using the Serkowski law of interstellar polarization (Serkowski et al. 1975). This is $P_\lambda/P_{\lambda\max} = e^{-K\ln^2(\lambda_{\max}/\lambda)}$. If the polarization is produced by aligned interstellar dust particles, the observed data (in terms of wavelength, *UBVRI*) will follow the formula given above, where each star is characterized by $P_{\lambda\max}$ and $\lambda_{\max}$.

Adopting $K = 1.66\lambda_{\max} + 0.01$ (Whittet et al. 1992), we have fitted our observations and computed the σ_1 parameter (the unit weight error of the fit) in order to quantify the departure of our data from the "theoretical curve" of Serkowski's law. A σ_1 value larger than 1.5 is considered an indication of the presence of a component of intrinsic stellar polarization. Another criterion of intrinsic stellar polarization is to compute the dispersion of the position angle for each star normalized by the average of the position angle errors ($\bar\epsilon$; Marraco, Vega, & Vrba 1993).

The $\lambda_{\max}$ values can also be used to test the origin of the polarization. In fact, since the average value of $\lambda_{\max}$ for the interstellar medium is 0.545 μm (Serkowski et al. 1975), objects showing $\lambda_{\max}$ much lower than this value are also candidates for having an intrinsic component of polarization (Orsatti, Vega, & Marraco 1998). The values we have obtained for $P_{\lambda\max}$, the σ_1 parameter, $\lambda_{\max}$, and $\bar\epsilon$, together with the identification of stars, are listed in Table 3.

Figure 2 shows the observed P_λ and θ_λ versus λ of those stars that are candidates for having an intrinsic component of polarization (stars 70, 73, and 254). For comparison purposes, the best Serkowski's law fit has been plotted as a continuous line. Star 220 also shows an intrinsic component of polarization on Table 2, but it is already known as a polarimetric variable. First Luna (1982) and then St-Louis et al. (1987) have made an extensive polarimetric study of this double-line binary (WC7+O5–8) system.

4.2. *Polarization Efficiency*

Figure 3 shows the plot of $P_{\lambda\max}$ versus E_{B-V} (Sung et al. 1998; Raboud et al. 1997; Baume et al. 1999) for each of the three groups. This plot is very useful for studying the polarization efficiency, defined as the ratio $P_{\lambda\max}/E_{B-V}$, which indicates how much polarization is obtained for a certain amount of extinction.

To understand the behavior of the polarimetry and the extinction, a detailed discussion of the distribution of the dust on the line of sight to the cluster is necessary. Neckel & Klare (1980) have studied the extinction values of the ISM and distances in our Galaxy using more than 11,000 stars. Their Figure 6*j*, which is the plot in the direction of NGC

TABLE 3
PARAMETERS OF THE SERKOWSKI FIT TO THE LINEAR POLARIZATION DATA FOR STARS IN NGC 6231

Stellar Identification	$P_{\max} \pm \epsilon_P$ (%)	σ_1	$\lambda_{\max} \pm \epsilon_{\lambda_{\max}}$ (mμ)	$\bar\epsilon$
1............................	0.846 ± 0.112	1.062	0.553 ± 0.189	18.9
6............................	0.355 ± 0.006	0.169	0.615 ± 0.027	10.4
16..........................	0.371 ± 0.023	0.338	0.542 ± 0.065	2.3
34..........................	1.511 ± 0.077	0.743	0.656 ± 0.064	12.2
70..........................	1.616 ± 0.274	5.933	0.627 ± 0.192	367.0
73..........................	1.953 ± 0.380	7.997	0.725 ± 0.220	199.5
80..........................	1.036 ± 0.031	0.577	0.551 ± 0.036	8.6
102........................	0.847 ± 0.011	0.236	0.581 ± 0.015	16.2
105........................	1.175 ± 0.027	0.538	0.493 ± 0.023	2.3
110........................	0.476 ± 0.075	0.932	0.427 ± 0.117	6.1
112........................	0.549 ± 0.018	0.463	0.536 ± 0.031	4.1
161........................	0.441 ± 0.141	1.612	0.321 ± 0.098	1.9
166........................	0.699 ± 0.031	0.209	0.439 ± 0.030	2.1
189........................	0.558 ± 0.131	0.629	0.377 ± 0.101	3.0
194........................	1.018 ± 0.371	0.987	0.205 ± 0.041	2.0
220........................	0.657 ± 0.024	0.360	0.506 ± 0.035	14.4
224........................	0.345 ± 0.027	0.624	0.507 ± 0.079	6.0
232........................	0.911 ± 0.018	0.220	0.484 ± 0.013	2.0
238........................	0.407 ± 0.028	0.451	0.549 ± 0.083	7.9
248........................	1.614 ± 0.043	0.350	0.468 ± 0.029	9.1
253........................	0.985 ± 0.044	0.524	0.480 ± 0.041	7.0
254........................	0.928 ± 0.078	0.867	0.460 ± 0.091	33.5
259........................	0.891 ± 0.035	0.566	0.472 ± 0.031	1.3
261........................	0.588 ± 0.017	0.257	0.450 ± 0.021	1.4
266........................	0.396 ± 0.024	0.709	0.589 ± 0.069	5.6
272........................	0.592 ± 0.063	0.643	0.382 ± 0.057	5.1
286........................	0.533 ± 0.118	0.864	0.348 ± 0.098	8.6
287........................	0.830 ± 0.012	0.207	0.474 ± 0.011	0.6
289........................	0.731 ± 0.032	0.788	0.439 ± 0.034	0.5
290........................	0.666 ± 0.012	0.163	0.469 ± 0.014	6.0
HD 152233.............	0.609 ± 0.066	0.926	0.514 ± 0.161	7.4
HD 152235.............	1.020 ± 0.021	0.386	0.465 ± 0.015	1.5
HD 152248.............	0.562 ± 0.029	0.462	0.533 ± 0.056	6.0
CPD −41 7733	0.444 ± 0.034	0.399	0.852 ± 0.095	5.6

6231, shows two steps in the absorption increase: the first one is very near to the Sun and associated with the Lupus cloud (Crawford 2000) at 150 pc ($A_V = 0.8$), and the second step is about 700–1000 pc and is also detected in the diffuse interstellar lines (Crawford 2001). This second step of absorption is responsible for $A_V \sim 0.6$. Baume et al. (1999) have reconstructed Neckel & Klare's plot with new CCD data and found a more complex structure obtaining a similar result for the distribution of dust between the Sun and the cluster. Nevertheless, Figure 7 of Baume et al. (1999) shows that NGC 6231 also has intracluster dust.

Most of the studies show that the cluster has differential reddening. For example, Sung et al. (1998) have made a bidimensional map of the distribution of E_{B-V} over the NGC 6231 cluster (see their Fig. 5). They show that the core of the cluster is less reddened and seems to lie in a hole in the reddening material ($E_{B-V} \sim 0.45$). To the south they find that the extinction increases to $E_{B-V} \sim 0.65$. The differential reddening of the cluster is extended, as discussed in Raboud et al. (1997) and Baume et al. (1999).

Figure 3 is the plot of $P_{\lambda\max}$ versus E_{B-V} for each group of stars. The upper panel are stars of the first group, the middle panel is for the second group of stars, and the bottom panel shows data of the third group of stars.
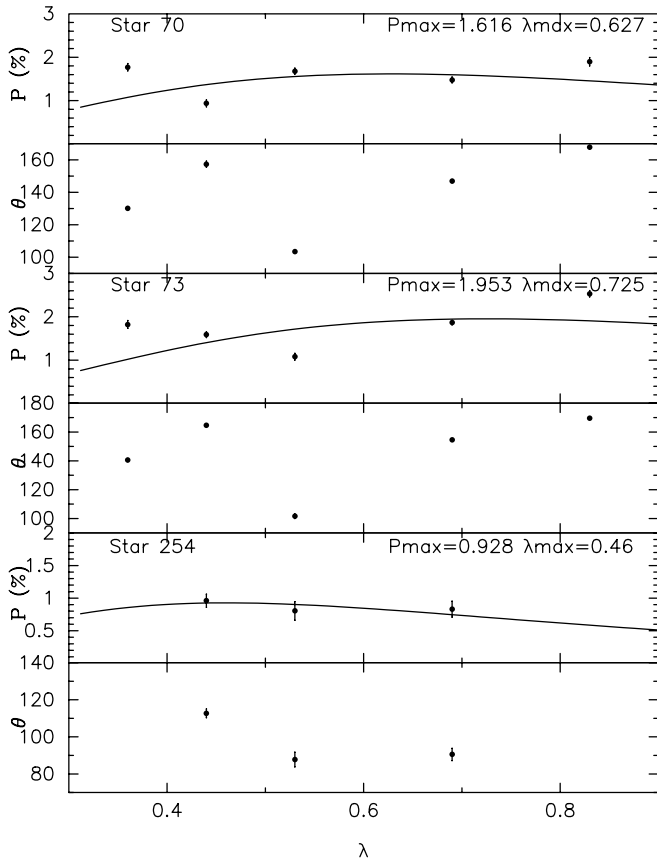
FIG. 2.—Plot of the observed data for objects showing large departures from the Serkowski law. *Solid line*: Best fit.

The solid line in the first panel of Figure 3 is the empirical upper limit relation for the polarization efficiency by the interstellar polarization $P_{\lambda\max} = R\,A_V = 9E_{B-V}$ (for normal dust, $R = 3.2$) given by Serkowski et al. (1975). The dashed line $(P_{\lambda\max}/E_{B-V} = 5)$ represents the observed
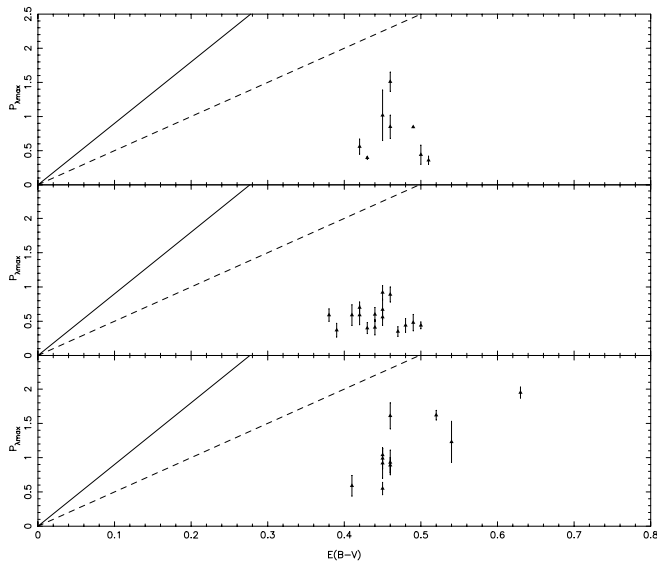

FIG. 3.—$P_{\lambda\max}$ vs. E_{B-V}. *Solid line*: $P_{\lambda\max} = 9E_{B-V}$. *Dashed line*: $P_{\lambda\max} = 5E_{B-V}$. *Top panel*: Stars of the first group. *Middle panel*: Second group. *Bottom panel*: Third group.

normal efficiency of the polarizing properties of the dust (Serkowski et al. 1975).

Although the observed data came from different sources and probably present large errors, some interesting properties can be appreciated from the figure. It is noticeable that all the groups have a polarizing efficiency lower than the $P_{\lambda\max}/E_{B-V} \sim 5$ expected. For an extinction of $E_{B-V} = 0.43$ (Baume et al. 1999) and the average polarization efficiency, the typical value should be around $P_{\lambda\max} \sim 2\%$. This value is much higher than the one observed in the cluster (see Table 3). Therefore, in all the groups, we have an important depolarization, and this effect is notorious for the stars of the semicircular structure (group 2) that have a much lower polarization than the first and third groups (see Fig. 3, *middle panel*). There are no stars with polarization greater than 0.95% in this group.

There is a question that remains to be answered: Why can we see this semicircular structure behind two layers of dust that orient the polarization vectors in different directions? It is pretty obvious that having only one dust layer on the line of sight would compose and change the direction of the polarization vectors, washing out this semicircular structure. On the other hand, the observed semicircular structure seems quite perfect. As we have discussed in the previous paragraph, in the particular case of NGC 6231, there are two layer of dust, a first one at Lupus (hereafter, the first component of extinction) and a second one in front of the cluster located at 1 kpc (Raboud et al. 1997; Baume et al. 1999; Neckel & Klare 1980), hereafter the second component. It is very important to notice that the two components are orthogonal and one of them can compensate for or diminish the other. The first component is dominated by dust in the Galactic plane, which has an angle of polarization of $\sim 45°$; the second component seems to be at right angles to the Galactic plane at $\sim 135°$. Figure 3 shows a huge depolarization for the second group of stars. We think that in the northern part the first component dominates the observed polarization, while in the south, the second component is the strong one. However, in the core, where the semicircular structure lies, both components (first and second) cancel each other, therefore making a polarization "window" through which we can observe inside the cluster. This interpretation also explains the depolarization of the stars located in the semicircular structure (second group).

We tested this interpretation of the extinction toward NGC 6231 by analyzing the polarization of the nonmembers stars. For example, in the first group, 102 is considered an F0 III star (Perry et al. 1991), so it must be located at about 379 pc from the Sun, and star 189 is a B9–8 V (Raboud et al. 1997) located at 1 kpc. Both stars are behind the Lupus cloud and have polarization angles similar to the direction of the Galactic disk. Therefore, we can deduce that the Lupus cloud is responsible for the polarization of the light in the direction of the Galactic disk. This cloud is reddening the stars behind it by $E_{B-V} = 0.25$ on average (Neckel & Klare 1980). For larger distances, Raboud et al. (1997) have found that the interstellar medium shows a relatively good transparency between 400 and 1000 pc.

Star 105 is also a nonmember star, but its polarization (and location in the cluster) is related to the third group of stars. Assuming that this star is a main-sequence object reddened by normal dust, it is possible to find an unique solution from the color-color diagram that gives an $E_{B-V} = 0.52$. This value is larger than the estimate for the

Lupus cloud and shows that this object is located behind another layer of dust that is polarizing the stellar light at right angles to the direction of the Galactic disk. Therefore, this star is probably located behind the second cloud at a distance of more than 1 kpc from the Sun.

4.3. The Semicircular Polarization Pattern

As depicted in Figure 1, the polarization vectors of the stars belonging to our second group (at the core of the cluster) displayed a semicircular pattern. This is very unlikely to be the result of a distribution of polarization angles at random, because the pattern is well organized. We think we are in the presence of an energetic phenomenon that has changed the magnetic field orientation, resulting in a realignment of the dust grains, which manifests itself in a rotation of the polarization vectors. We propose that a supernova event occurred some time ago and produced a shock over the ISM. It pushed the gas and dust (and the associated magnetic field), causing the dust grains to reorient to the new direction of the magnetic field. We will discuss in the next paragraphs the relevant questions associated with the proposed supernova event.

Where did this phenomenon occur? Tracing lines perpendicular to the most conspicuous polarimetric vectors, it is possible to obtain an approximate center at the crossing point where these lines overlap each other. This center seems to be at $\alpha = 16^h54^m22^s$, $\delta = -41°46'30''$ (J2000.0; Fig. 4). This semicircle is very regular, and the vectors converge clearly to a center. We think this is a solid argument for the existence of the center of this pattern, which means that the energetic phenomenon was produced at a certain fixed location in the cluster. This supports the idea that a supernova exploded in the near past of the cluster, located at the center of the crossing lines, as shown in Figure 4.

Could a supernova event have happened in NGC 6231? The earliest star on the main sequence, not considering

binaries, is at present of spectral type O9 (292, HD 326329), and there is evidence of more massive stars that evolved off of the main sequence (Baume et al. 1999). Therefore, it is very probable that a star more massive than HD 326329 evolved to a supernova stage in the past. Also, Baume et al. (1999) computed the initial mass function (IMF) of NGC 6231 with binary correction and obtained a slope of $x = 1.14 \pm 0.10$ for $x = \log(dN/\delta M)/\log(M)$. This slope of the distribution allows the existence of a former star of about 70 $M_\odot$ (an O3–O4) without any change in the parameters of the observed IMF. This means that one or a few (because we are dealing with small-number statistics) very massive stars could have lived in the past with no contradiction with the actual IMF. So the evolutionary status of the cluster population in NGC 6231 indicates that some massive stars evolved and probably became supernovae.

Is there other evidence on the ISM of this supernova event? Crawford and collaborators (Crawford, Barlow, & Blades 1989; Crawford 1989, 1992, 2001) have made a very detailed study of the interstellar lines (Na I, Ca II, and K I) toward Sco OB1. Although these studies are related to the whole Sco OB1 association, this series of papers includes the analysis some of the brightest stars of NGC 6231. They have found several components and classified them into three major groups (Crawford 2001). The first one consists of several components with radial velocities in the range $-20 \leq v_{helio} \leq 6$ km s^{-1}, which are consistent with the Galactic rotation along the 1900 pc to Sco OB1. All the clouds in this component are presumably foreground and unrelated to Sco OB1. For example, components in the velocity range $-6 \leq v_{helio} \leq 6$ km s^{-1} are probably associated with the Lupus molecular cloud complex at a distance of 150 pc.

The second group of interstellar lines found by Crawford (2001, and references therein) is the "shell component," which has velocities more negative than -20 km s^{-1} (-22 km s^{-1} is the velocity expected for the Galactic rotation model at a distance of 1900 pc) and these clouds of interstellar matter seem to be related with the shells surrounding the Sco OB1 association. In a previous work, Crawford et al. (1989) found a very low Na I/Ca II relation in this component. This finding was explained by the removal of the Ca atoms from the grain surfaces by shock velocities of ≥ 20 km s^{-1}. New data (Crawford 2001) indicate that the observed shell component has an upper limit for the temperature on the order of $T = 450°$ K (as observed in the spectrum of HD 152235, a member of NGC 6231), which is low for a postshock temperature ($T \geq 10^4$). However, as Crawford (2001) noted, the cooling time of a shock for the regular interstellar medium ($v_s = 20$ km s^{-1}, $n_H = 10$ cm^{-3}) gives $t_{cool} = 6300$ yr; meanwhile, the depletion timescale for the Ca to become part of the interstellar grains is $t_{dep} = 1.6 \times 10^7$ yr. Therefore, shocks in the near past can account for the low Na I/Ca II observed in the interstellar lines.

The third component of interstellar line has velocities more positive than those predicted by the Galactic rotation models. In NGC 6231, HD 152249 exhibits an interstellar absorption component at a velocity of $+19$ km s^{-1}. Note that HD 152249 is located in the core of the NGC 6231 and 1' to the south of the semicircular polarization pattern. This component has a low Na I/Ca II ratios (≤ 0.4), which (as described above) is an indication of shock. This component could be located near the Sun in the Upper Centarus Lupus,
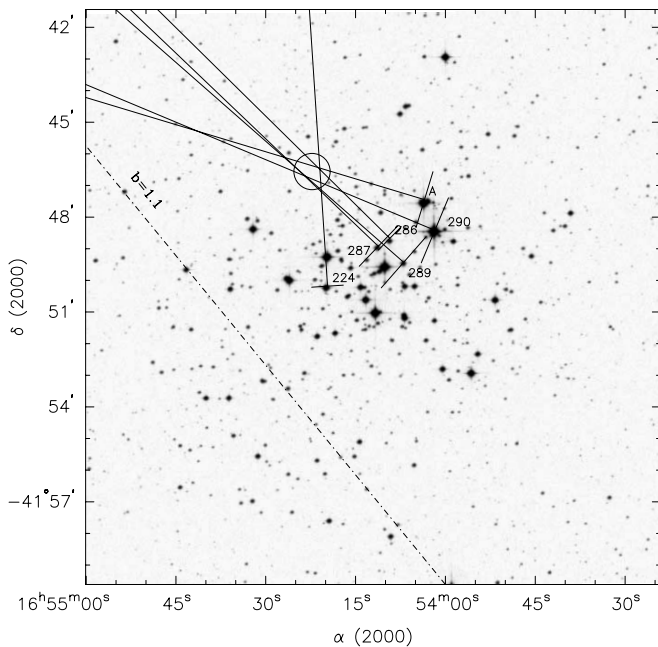

Fig. 4.—Straight lines from the stars are perpendicular to their polarization vectors. These lines seem to converge to a center. Star A is HD 152248.

or it could be an expanding interstellar structure related to NGC 6231.

Both the second and third interstellar components exhibit the low Na I/Ca II ratio and, in our opinion, this is a strong support for shocks in the region and gives clues over a turbulent scenario in the near past of NGC 6231. These interstellar line components are probably located in the cluster, as discussed by Crawford in his series of papers, and were produced by shocks in the region. Crawford's point of view is consistent with our interpretation of polarimetric observations.

Sung et al. (1998), studying the PMS stars in NGC 6231, have found a discontinuity in the number of stars near the MS band with ages between 30 and 12 Myr. They have suggested that probably some PMSs are not Hα emitters, and they are not detected by the typical $R-$Hα versus $V-I$ diagram. They explained the lack of Hα emission by suggesting that all the material surrounding the PMS stars, material that would normally produce strong Hα emission, could be swept away by stellar winds from massive stars, Wolf-Rayet stars, or past supernova explosions. Their result is also compatible with and a strong support to our polarimetric findings.

Other interesting results showing some clues to support the idea of energetic events on the cluster NGC 6231 came from Manchanda et al. (1996). To explain the *COS B* diffuse emission of gamma-ray observations, Manchanda et al. (1996) propose that strong winds in the cluster interact with the ISM, creating the suitable condition for cosmic-ray enhancement.

5. OTHER POSSIBLE EXPLANATIONS OF THE SEMICIRCULAR POLARIZATION PATTERN

We have proposed a supernova event to explain our observations, but we have analyzed other possible interpretations. For example, a loop in the magnetic field would lead to similar observations; however, several papers (Neckel & Klare 1980; Baume et al. 1999) show very clearly that the dust along the line of sight is distributed in layers, and there is no dust between these layers. Thus, there is not a continuum of dust to be aligned by the magnetic field. Therefore, we have discarded this interpretation of the semicircular polarization pattern.

Other explanations for the observed polarization pattern might not require a supernova. Same observed bubbles in the Milky Way are supposed to be made by the strong winds of Wolf-Rayet stars over a long period of time. In some of these interstellar bubbles, such as WR 101 (Cappa, Goss, & Pineault 2002), the Wolf-Rayet star appears to be located in an eccentric position close to the densest part of the nebula. This phenomenon could be explained by an inhomogeneous structure of the ISM near the Wolf-Rayet star or from the motion of the star inside the shell (Cappa et al. 2002). This would be the case if the Wolf-Rayet star 220 (HD 152270) is responsible for the bubble in NGC 6231. The location of this star is eccentric to the semicircular pattern.

6. SUMMARY

We have observed multicolor (*UBVRI*) linear polarization (*P* and θ) for 35 of the stars in the direction of NGC 6231. We have found a very unusual distribution of the angles of the polarization vectors. To the north of the cluster, the polarization angles are dominated by the direction of the Galactic disk; to the south, they are perpendicular to this orientation. Close to the core of the cluster, the polarization vectors are well organized in a regular pattern, showing a semicircular morphology, which we interpret as a reorientation of the dust particles by the magnetic field.

We suppose that an energetic event (very probably a supernova) occurred some time ago and produced a shock pattern in the local ISM. A supernova is compatible with the evolutionary status of the cluster. We discuss in this paper independent confirmations of this event from studies of the interstellar lines (Crawford 2001) to the photometric results of the PMS stars given by Sung et al. (1998).

REFERENCES

Balona, L. A., & Laney, C. D. 1995, MNRAS, 276, 627
Baume, G., Vázquez, R. A., & Feinstein, A. 1999, A&AS, 137, 233
Cappa, C. E., Goss, W. M., & Pineault, S. 2002, AJ, 123, 3348
Crawford, I. 1989, MNRAS, 241, 575
———. 1992, MNRAS, 259, 47
———. 2000, MNRAS, 317, 996
———. 2001, MNRAS, 328, 1115
Crawford, I., Barlow, M. J., & Blades, J. C. 1989, ApJ, 336, 212
Feinstein, C., Baume, G., Vázquez, R., Virpi, N., & Cerruti, M. G. 2000, AJ, 120, 1906
Feinstein, C., Baume, G., Vergne, M., & Vázquez, R. 2003, A&A, 409, 933
Luna, H. 1982, PASP, 94, 695
Manchanda, R. K., et al. 1996, A&A, 305, 457
Maronna, R., Feinstein, C., & Clocchiatti, A. 1992, A&A, 260, 525
Marraco, H. G., Vega, E., & Vrba, F. J. 1993, AJ, 105, 258

Mermilliot, J. C., & Maeder, A. 1986, A&A, 158, 45
Neckel, Th., & Klare, G. 1980, A&AS, 42, 251
Orsatti, A. M., Vega, E., & Marraco, H. G. 1998, AJ, 116, 226
Perry, C. L., Hill, G., & Christodoulou, D. M. 1991, A&AS, 90, 195
Raboud, D., Cramer, N., & Berneasconi, P. A. 1997, A&A, 325, 167
Scaltriti, F., Cellino, A., Anderlucci, E., Corcione, L., & Piirola, V. 1989, Soc. Astron. Italiana Memorie, 60, 243
Seggewiss, W. 1968, Veröff. Astron. Inst. Bonn, 79, 33
Serkowski, K., Mathewson, D. L., & Ford, V. L. 1975, ApJ, 196, 261
Shobbrook, R. R. 1983, MNRAS, 205, 1229
St-Louis, N., Drissen, L., Moffat, A. F. J., Bastien, P., & Tapia, S. 1987, ApJ, 322, 870
Sung, H., Bessell, M. S., & Lee, S. W. 1998, AJ, 115, 734
Waldhausen, S., Martínez, R., & Feinstein, C. 1999, AJ, 117, 2882
Whittet, D. C. B., Martin, P. G., Hough, J. H., Rouse, M. F., Nailey, J. A., & Axon, D. J. 1992, ApJ, 386, 562